SPANDIDOS PUBLICATIONS

EXPERIMENTAL AND THERAPEUTIC MEDICINE 19: 557-568, 2020

The preventive effect of *Apocynum venetum* polyphenols on D-galactose-induced oxidative stress in mice

HUAN GUO[1*], ZHIPING KUANG[1*], JING ZHANG[2], XIN ZHAO[3], PING PU[1] and JUNFENG YAN[4]

[1]The First Department of Orthopaedic Surgery, Chongqing Traditional Chinese Medicine Hospital, Chongqing 400021; [2]Environment and Quality Inspection College, Chongqing Chemical Industry Vocational College, Chongqing 401228; [3]Chongqing Collaborative Innovation Center for Functional Food, Chongqing University of Education, Chongqing 400067; [4]Department of Internal Medicine-Neurology, Chongqing Traditional Chinese Medicine Hospital, Chongqing 400021, P.R. China

Received February 4, 2019; Accepted November 5, 2019

DOI: 10.3892/etm.2019.8261

Abstract. *Apocynum venetum* is a traditional medicine that is rich in polyphenols. *Apocynum venetum* polyphenol extract (AVP) contains the active substances neochlorogenic acid, chlorogenic acid, rutin, isoquercitrin, astragaloside and rosmarinic acid. In the present study, the preventive effect of AVP against D-galactose-induced oxidative stress was studied in a mouse model. The sera, skin, livers and spleens of mice were examined using hematoxylin and eosin staining, reverse transcription-quantitative PCR and western blot analysis. The biochemical results showed that AVP improved the thymus, brain, heart, liver, spleen and kidney indices in a mouse model of oxidative stress. AVP was also able to reverse the reduction in levels of superoxide dismutase (SOD), glutathione peroxidase and glutathione, and increased the levels of nitric oxide and malondialdehyde identified in the serum, liver, spleen and brain of mice exposed to oxidative stress. Pathological observations confirmed that AVP could inhibit oxidative damage to the skin, liver and spleen of mice caused by D-galactose. Further molecular biological experiments also demonstrated that AVP increased the expression of neuronal nitric oxide synthase, endothelial nitric oxide synthase, Cu/Zn-SOD, Mn-SOD, catalase, heme oxygenase-1, nuclear factor-erythroid 2-related factor 2, γ-glutamylcysteine synthetase and NAD(P)H quinone dehydrogenase 1 and reduced the expression of inducible nitric oxide synthase in the liver and spleen of treated mice compared to controls. Notably, the preventive effect of AVP against D-galactose-induced oxidative damage in mice was better than that of the confirmed antioxidant vitamin C. In conclusion, AVP exhibited an antioxidant effect and the AVP-rich *Apocynum venetum* may be considered a plant resource with potential antioxidative benefits.

Correspondence to: Professor Ping Pu, The First Department of Orthopaedic Surgery, Chongqing Traditional Chinese Medicine Hospital, Panxi 7 Branch Road 6, Chongqing 400021, P.R. China
E-mail: 18983723386@163.com

Professor Junfeng Yan, Department of Internal Medicine-Neurology, Chongqing Traditional Chinese Medicine Hospital, Panxi 7 Branch Road 6, Chongqing 400021, P.R. China
E-mail: yjfmail2002@sina.com

*Contributed equally

Key words: *Apocynum venetum*, polyphenol, D-galactose, oxidation, Cu/Zn-superoxide dismutase expression

Introduction

Apocynum venetum L. (*A. venetum*), a genus of the plant family Apocynaceae, is distributed throughout the temperate regions of Eurasia and North America (1). The dried leaves of *A. venetum* are used as treatments in traditional Chinese medicine (TCM) and also as a tea. *A. venetum* leaves have been suggested to lower cholesterol and blood pressure, and are prescribed in TCM for sedation, as antidepressants and as anti-anxiety treatments, due to the reported action of *A. venetum* on the nervous system (2). *A. venetum* has also been reported to exert an antioxidative effect, the mechanism of which is thought to be related to free radical scavenging and diuresis (2-5). The polyphenols found in *A. venetum* leaves potentially represent a new class of active ingredients (2).

Oxidative stress is an endogenous process that gradually damages the body. Oxidative stress aggravates various diseases, including hypertension, type 2 diabetes mellitus, atherosclerosis and dementia (6-8). Excessive redox-active species and free radicals can also cause oxidative damage of biological macromolecules, which leads to oxidative stress in the body. Oxidative stress promotes the production of hydrogen peroxide in mitochondria, which in turn increases oxidative damage (9). Redox regulation is an important focus in the study of oxidative stress. Maintaining the redox balance and regulating redox-related genes are important strategies to alleviate oxidative stress (10).

D-galactose is a commonly used aging-inducing agent in research that can be used to establish animal models of oxidative stress. A small amount of D-galactose can be converted to glucose and metabolized by the body. However, excessive D-galactose leads to a disordered cellular metabolism, alters

the activity of oxidase in tissues and cells, and produces a large number of superoxide anions and oxidative products, which results in oxidative damage to both the structure and function of biological macromolecules (11). The oxidation model of D-galactose has been established to verify the antioxidant effect of antioxidant active substances. This model has been utilized in the research and development of antioxidant health products (12).

A previous study indicated that plant polyphenols have antioxidant and free radical scavenging capacities, due to their structural characteristics. The phenolic hydroxyl structure, particularly the ortho-phenolic hydroxyl in catechol or pyrogallol, is easily oxidized to a quinone structure; this makes it capable of capturing free radicals, such as reactive oxygen species (2). This structure can reduce or prevent the oxidation reaction in tissues by binding to lipid free radicals produced in oxidation (13). Plant polyphenols have also been shown to exert antioxidative effects in animals and humans in clinical studies (14,15). Plant polyphenols act as antioxidants via increases in the activities of three important antioxidant enzymes: Superoxide dismutase (SOD), glutathione (GSH) peroxidase (GSH-Px) and catalase (CAT) (16).

In the present study, *A. venetum* polyphenol extract (AVP) was extracted and was administered to mice subjected to D-galactose-induced oxidative stress. The effects of AVP on the serum and tissues of oxidized mice were observed, and the mechanism of AVP-induced prevention of oxidation was studied through the detection of oxidative stress-related genes. This study provides a theoretical basis for further research into the use of AVP as a medical treatment.

Materials and methods

Extraction of AVP. Briefly, 500 g *A. venetum* (Huake Ecology Agriculture & Forestry Technology Co., Ltd.) was crushed into a fine powder. Ethanol solution (50 ml; volume ratio: 45%) was added to the powder for mixing and extraction at 90˚C for 30 min using a vortex shaker (TRS 140, Shanghai Brave Construction Development Co., Ltd; Shanghai Dam Industrial Co., Ltd.). After three rounds of extraction and the mixing, the pH of the extract was adjusted to 6.0 using 2.877 mol/l HCl. A mixed precipitant of $AlCl_3$ (30 g) and $ZnCl_2$ (60 g) was added (in a volume of 800 ml) to the extract for precipitation, followed by centrifugal separation at 1,700 x g for 10 min at 25˚C. Hydrochloric acid (volume ratio: 12%; 1 l) was added to the precipitate after centrifugation. The supernatant was separated using a separating funnel, and then, 100 ml ethyl acetate was added twice for extraction by vortex shaker. The extract was then subjected to rotary evaporation to obtain AVP, as previously reported (17).

High-performance liquid chromatography (HPLC). HPLC was performed using the Ultimate 3000 system (Thermo Fisher Scientific, Inc.). The reference substances neochlorogenic acid, chlorogenic acid, rutin, isoquercitrin, astragaloside and rosmarinic acid (20 mg of each substance; Shanghai Yuanye Bio-Technology Co., Ltd.) were weighed and added to methanol at a chromatographic level of 2 ml. The reference substances were dissolved by full oscillation and reference substance reserve solutions were obtained. The two mobile phase solvents were: Mobile phase A, 0.5% acetic acid water; mobile phase B, acetonitrile. The flow rate was 0.5 ml/min. Accucore™ C18 chromatography columns (particle size 2.6 μm; dimensions, 4.6x150 mm; Thermo Fisher Scientific, Inc.) were used. The injection volume was 10 μl and the column temperature was 30˚C. The detection wavelength was 328 nm and the gradient conditions 0-30 min, 12-45% (phase B); 30-35 min, 45-100% (phase B); 35-40 min, 100% (phase B) were used to determine the components of the AVP.

Animal oxidation experiment. A total of 50 specific-pathogen-free-grade Institute of Cancer Research mice (age, 6 weeks; weight, 25±2 g; 25 male and 25 female) were allowed 1 week to adapt to a temperature of 25±2˚C and a relative humidity of 50±5%. All mice received a normal diet and food and water were freely available. The mice were then divided into the following five groups: Control group, model group, AVP low-concentration (AVP-L) group, AVP high-concentration (AVP-H) group, and vitamin C (Vc) group. There were 10 mice (5 male and 5 female) per group.

During the first 4 weeks, mice in the model group and the control group received normal diet and drinking water, and each mouse received 0.2 ml saline per day by gavage. Mice in the AVP-L and AVP-H groups were treated with AVP at 50 or 100 mg/kg once per day by gavage. Mice in the Vc group were treated with Vc (Hefei Bomei Biotechnology Co., Ltd.) at 100 mg/kg daily by gavage. After 4 weeks, mice in the groups other than the control group were intraperitoneally injected with D-galactose (Hefei Bomei Biotechnology Co., Ltd.) at a concentration of 120 mg/kg once per day for 6 weeks. At the same time, mice in the AVP-L, AVP-H and Vc groups were also treated with AVP and Vc once per day for 6 weeks by gavage, whereas mice in the model group and the control group received the equivalent dose of saline (12). At 10 weeks, all mice were sacrificed after 24 h of fasting. Mice were euthanized using cervical dislocation. Blood samples were collected from heart and liver tissues and stored until further experiments. The organ indices of the thymus, brain, heart, liver, spleen and kidney were measured, as follows: Organ index=organ mass (g)/body mass of mouse (kg) x100. These experiments followed a protocol approved by the Animal Ethics Committee of Chongqing Collaborative Innovation Center for Functional Food (approval no. 200802002B).

Determination of nitric oxide (NO) and malondialdehyde (MDA) concentration, and SOD and GSH-Px activity in serum and liver tissues. Mouse blood (0.1 ml) was centrifuged at 2,100 x g for 10 min at 25˚C and the serum was collected. The concentrations of NO (A012-1-2) and MDA (A003-1-2), and the activities of SOD (A001-3-2) and GSH-Px (A005-1-2) in the serum were determined using their respective kits, following the instructions of the manufacturers (Nanjing Jiancheng Bioengineering Institute). In addition, a total of 2 g liver and brain tissue was placed into a glass homogenate tube, 18 ml saline was added into the homogenate tube, and the homogenate was ground up and down at 2,100 r/min using a tissue masher (TENLIN-C; Jiangsu Tianling Instrument Co., Ltd.) for 10 min to produce a 10% homogenate of liver and brain tissues. The concentrations of NO and MDA, and

the activities of SOD and GSH-Px were determined in these homogenates, using the aforementioned kits.

Observation of skin, liver and spleen tissues. Approximately 0.5 cm^2 skin, liver and spleen tissues of mice were removed and fixed in 10% formalin solution for 48 h at 4˚C. Skin, liver and spleen tissues were dehydrated gradually through 70, 80, 90% and anhydrous ethanol, and the tissues were paraffin wax embedded sectioned (10 μm) and permabilized for hematoxylin and eosin (H&E) staining for 25 min at 25˚C. Morphological changes in the tissues were observed (x100) under an optical microscope (BX43; Olympus Corporation). A section was prepared from the skin, liver and kidney of each mouse and 3 fields of view were imaged per section.

Reverse transcription-quantitative PCR (RT-qPCR). The skin, liver and spleen tissues (0.1g) of mice were crushed using a tissue masher (TENLIN-C, Jiangsu Tianling Instrument Co., Ltd.) RNAzol® (Sigma-Aldrich; Merck KGaA) was used to extract total RNA from tissues, and the concentration of the extracted total RNA was diluted to 1 μg/μl. Subsequently, 5 μl diluted total RNA solution was collected, and RT was conducted according to the instructions of the RT kit (Tiangen Biotech Co., Ltd.) to obtain the cDNA template at 25˚C. cDNA template (2 μl) was mixed with 10 μl SYBR Green PCR Master Mix (Thermo Fisher Scientific, Inc.) and 1 μl upstream and downstream primers (Table I). The reaction conditions were as follows: 95˚C for 60 sec, followed by 40 cycles of 95˚C for 15 sec and 55˚C for 30 sec followed by a final step at 72˚C for 35 sec. A StepOnePlus Real-Time PCR system (Thermo Fisher Scientific, Inc.) was used for qPCR. GAPDH was used as an internal reference. The $2^{-\Delta\Delta Cq}$ method was used to determine the relative gene expression (18).

Table I. Primer sequences.

Gene name	Sequence (5'-3')
nNOS	Forward: ACGGCAAACTGCACAAAGC
	Reverse: CGTTCTCTGAATACGGGTTGTTG
eNOS	Forward: TCAGCCATCACAGTGTTCCC
	Reverse: ATAGCCCGCATAGCGTATCAG
iNOS	Forward: GTTCTCAGCCCAACAATACAAGA
	Reverse: GTGGACGGGTCGATGTCAC
Cu/Zn-SOD	Forward: AACCAGTTGTGTTGTCAGGAC
	Reverse: CCACCATGTTTCTTAGAGTGAGG
Mn-SOD	Forward: CAGACCTGCCTTACGACTATGG
	Reverse: CTCGGTGGCGTTGAGATTGTT
CAT	Forward: GGAGGCGGGAACCCAATAG
	Reverse: GTGTGCCATCTCGTCAGTGAA
HO-1	Forward: ACAGATGGCGTCACTTCG
	Reverse: TGAGGACCCACTGGAGGA
Nrf2	Forward: CAGTGCTCCTATGCGTGAA
	Reverse: GCGGCTTGAATGTTTGTC
γ-GCS	Forward: GCACATCTACCACGCAGTCA
	Reverse: CAGAGTCTCAAGAACATCGCC
NQO1	Forward: CTTTAGGGTCGTCTTGGC
	Reverse: CAATCAGGGCTCTTCTCG
GAPDH	Forward: AGGTCGGTGTGAACGGATTTG
	Reverse: GGGGTCGTTGATGGCAACA

γ-GCS, γ-glutamylcysteine synthetase; CAT, catalase; eNOS, endothelial nitric oxide synthase; HO-1, heme oxygenase-1; iNOS, inducible nitric oxide synthase; nNOS, neuronal nitric oxide synthase; Nrf2, nuclear factor-erythroid 2 related factor 2 NQO1, NAD(P)H quinone dehydrogenase 1; SOD, superoxide dismutase.

Western blotting. Liver tissue (100 mg) was homogenized in 1 ml RIPA buffer (Thermo Fisher Scientific, Inc.) containing 10 μl phenylmethylsulfonyl fluoride, and centrifuged at 6,700 x g at 4˚C for 5 min. The middle protein layer was taken to measure the protein concentration using a bicinchoninic acid kit (Bio-Rad Laboratories, Inc.). The samples were diluted to 50 μg/μl, mixed with sample buffer (4:1) and heated at 100˚C for 5 min. SDS-PAGE (12%) was carried out and 10 μg of protein was loaded per lane and proteins were transferred onto a PVDF membrane. Membranes were blocked in TBS-0.05% Tween (TBST) containing 5% skim milk for 1 h at 25˚C. After blocking, the membrane was incubated at 25˚C for 2 h with primary antibodies against Cu/Zn-SOD (cat. no. PA5-270240; 1:1,000), Mn-SOD (cat. no. LF-MA0030; 1:1,000) and beta-actin (cat. no. MA5-15739; 1:1,000). The membrane was then washed with TBST and incubated at 25˚C for 1 h with secondary antibody (cat. no. A32723; 1:500) (17). All antibodies were supplied by Thermo Fisher Scientific, Inc. SuperSignal™ West Pico Plus was used to visualize proteins by iBright FL1000 (both Thermo Fisher Scientific, Inc.). ImageJ version 1.44 (National Institutes of Health) was used for semi-quantitative analysis of protein expression.

Statistical analysis. Serum and tissue experiments were conducted three times in parallel with each mouse, and the mean values were obtained. SAS® version 9.1 statistical software (SAS Institute, Inc.) was used to analyze the data. One-way ANOVA followed by Tukey's test was used for multiple comparisons. $P<0.05$ (alpha level) was considered to indicate a statistically significant difference (19).

Results

AVP component analysis. Analysis by HPLC identified that AVP contained six known chemical constituents, namely neochlorogenic acid, chlorogenic acid, rutin, isoquercitrin, astragalin and rosmarinic acid (Fig. 1). Among them, isoquercitrin made up the greatest proportion, followed by neochlorogenic acid and chlorogenic acid (Table II).

Organ indices of mice. As shown in Table III, mice in the control group had the highest indices in the thymus, brain, heart, liver, spleen and kidney, whereas mice in the model group had the lowest organ indices. Both AVP and Vc significantly increased organ indices when compared with the model group ($P<0.05$). The effect of AVP appeared superior to that of Vc at the same concentration. These data suggested that AVP could inhibit the decline of organ indices caused by oxidative stress-induced tissue atrophy.

Levels of NO, SOD, GSH-Px, GSH and MDA. As shown in Tables IV-VII, mice in the control group exhibited the stron-

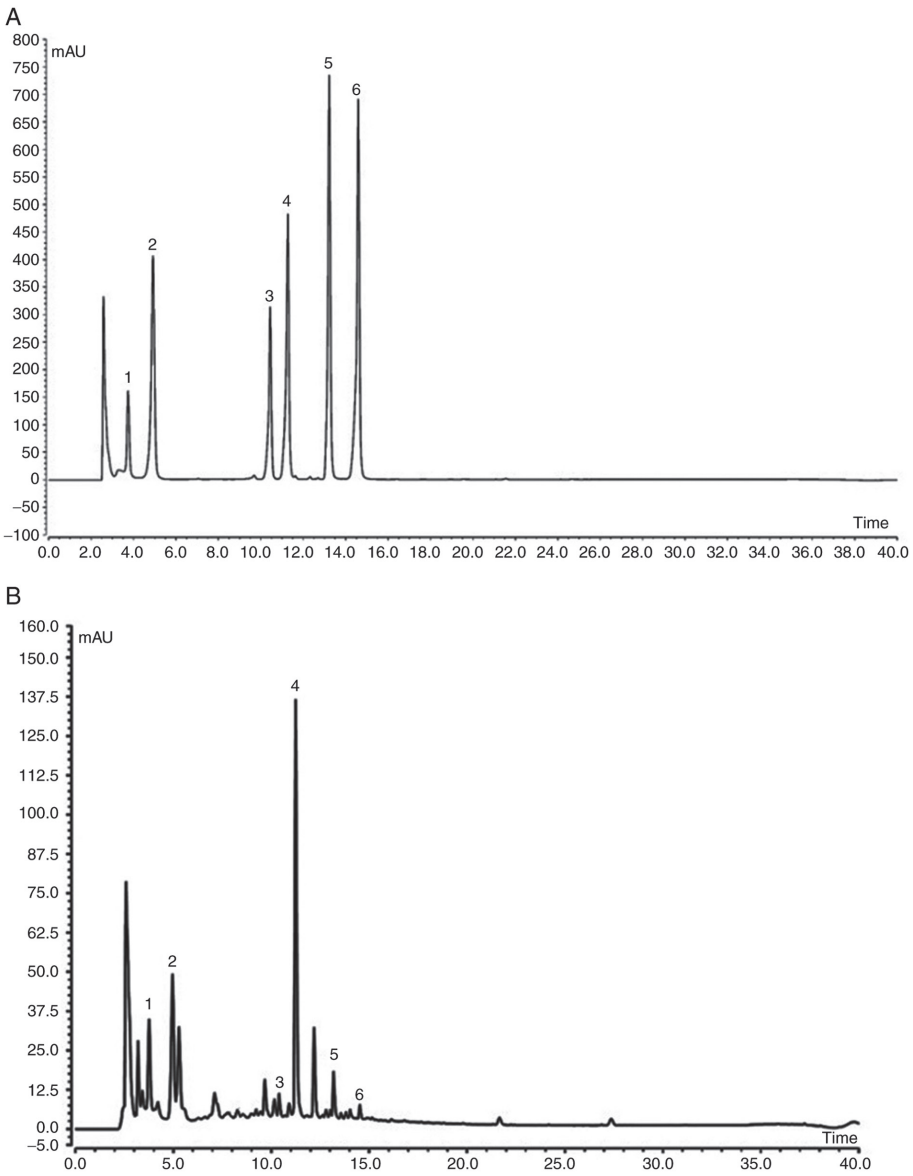

Figure 1. Constituents of *Apocynum venetum* polyphenol extract. (A) Standard chromatogram. (B) AVP chromatogram. 1, neochlorogenic acid; 2, chlorogenic acid; 3, rutin; 4, isoquercitrin; 5, astragalin; 6, rosmarinic acid; AVP, *Apocynum venetum*.

gest SOD, GSH-Px and GSH activity, and the lowest NO and MDA levels in the serum, liver, spleen and brain compared with the other groups. Mice in the model group had the lowest levels compared with the other groups. Following AVP treatment, SOD, GSH-Px and GSH activities in mice were significantly increased compared with the model group ($P<0.05$), whereas NO and MDA levels were significantly decreased ($P<0.05$). The aforementioned indicators improved until they were close to those of the control group following AVP-H treatment, and the effect was markedly better than that of Vc.

Observation of the mice livers and spleens. As shown in Fig. 2, the epidermal structure of normal mice was complete and clear, and the dermis was rich in collagen fibers. The boundary between the dermis and epidermis was clear and the number of fat vacuoles was normal. In the model group, the amount of collagen fibers in the skin was very low and numerous fat vacuoles were visible. The dermis was inflammatory cells infiltrated, and the boundary between the dermis and the epidermis was unclear. AVP treatment reduced the large number of fat vacuoles caused by D-galactose, alleviated the phenomenon of infiltration, and allowed the boundary between epidermis and dermis to remain clear.

Table II. Constituents of *Apocynum venetum* polyphenol extract.

Substance	Concentration (mg/ml)
Neochlorogenic acid	9.98
Chlorogenic acid	4.94
Rutin	0.81
Isoquercitrin	10.87
Astragalin	0.78
Rosmarinic acid	0.21

Table III. Organ indices of mice in each group (n=10).

Group	Thymus index	Brain index	Cardiac index	Liver index	Spleen index	Kidney index
Normal	0.29±0.04[b]	5.13±0.22[b]	3.57±0.19[b]	23.12±1.13[b]	1.65±0.11[a]	4.50±0.30[b]
Model	0.16±0.3	3.34±0.20	1.95±0.19	17.17±0.97	1.00±0.10	2.79±0.17
Vc	0.23±0.02[a]	4.43±0.20[b]	2.88±0.09[a]	20.90±0.90[a]	1.45±0.10[a]	3.89±0.15[a]
AVP-L	0.20±0.04[a]	3.79±0.16[a]	2.46±0.10[a]	19.47±1.05[a]	1.32±0.08[a]	3.54±0.23[a]
AVP-H	0.26±0.02[a]	4.75±0.22[b]	3.14±0.16[b]	21.92±0.98[a]	1.54±0.08[a]	4.13±0.17[b]

Values are presented as the mean ± standard deviation (N=10/group). [a]P<0.05 and [b]P<0.01 vs. the model group. Vc, mice treated with Vc (100 mg/kg); AVP-L, mice treated with a low concentration of AVP (50 mg/kg); AVP-H, mice treated with a high concentration of AVP (100 mg/kg). AVP, *Apocynum venetum* polyphenol extract; Vc, vitamin C.

Table IV. Levels of NO, SOD, GSH-Px, GSH and MDA in the serum of mice (n=10).

Group	NO (μmol/l)	SOD (U/ml)	GSH-Px (U/ml)	GSH (mg/l)	MDA (nmol/ml)
Normal	19.90±0.62[b]	220.71±8.13[b]	212.09±5.05[b]	46.07±2.60[b]	3.91±0.36[b]
Model	60.83±1.04	65.20±1.44	73.39±3.11	11.41±0.56	41.60±1.29
Vc	34.47±0.80[b]	159.41±4.17[b]	136.67±4.26[a]	29.80±0.91[a]	19.03±1.17[b]
AVP-L	47.89±0.40[a]	97.60±3.41[a]	102.97±3.32[a]	20.69±0.71[a]	28.61±1.33[a]
AVP-H	26.42±0.44[b]	190.37±4.77[b]	175.63±4.43[b]	37.02±1.64[b]	11.03±0.20[b]

Values are presented as the mean ± standard deviation (n=10/group). [a]P<0.05 and [b]P<0.01 vs. the model group. Vc, mice treated with Vc (100 mg/kg); AVP-L, mice treated with low concentration of AVP (50 mg/kg); AVP-H, mice treated with a high concentration of AVP (100 mg/kg). AVP, *Apocynum venetum* polyphenol extract; GSH, glutathione; GSH-Px, glutathione peroxidase; MDA, malondialdehyde; NO, nitric oxide; SOD, superoxide dismutase; Vc, vitamin C.

Table V. Levels of NO, SOD, GSH-Px, GSH and MDA in the liver of mice (n=10).

Group	NO (μmol/l)	SOD (U/ml)	GSH-Px (U/ml)	GS (mg/l)	MDA (nmol/ml)
Normal	2.12±0.06[b]	95.49±2.63[b]	204.82±17.28[b]	9.57±0.48[b]	1.13±0.09[b]
Model	9.34±0.17	22.86±1.21	71.20±5.18	3.20±0.21	8.95±0.20
Vc	5.48±0.29[a]	52.94±1.81[a]	125.92±2.85[a]	6.33±0.15[a]	3.05±0.12[a]
AVP-L	7.26±0.29[a]	34.92±1.95[a]	89.89±1.85[a]	4.59±0.26[a]	5.49±0.33[a]
AVP-H	3.98±0.08[a]	75.86±2.01[b]	148.54±2.13[b]	7.56±0.28[b]	2.19±0.14[b]

Values are presented as the mean ± standard deviation (N=10/group). [a]P<0.05 and [b]P<0.01 vs. the model group. Vc, mice treated with Vc (100 mg/kg); AVP-L, mice treated with low concentration of AVP (50 mg/kg); AVP-H, mice treated with a high concentration of AVP (100 mg/kg). AVP, *Apocynum venetum* polyphenol extract; GSH, glutathione; GSH-Px, glutathione peroxidase; MDA, malondialdehyde; NO, nitric oxide; SOD, superoxide dismutase; Vc, vitamin C.

As shown in Fig. 3, in the control group, hepatic cell chords were radially arranged around the central vein, with a regular morphology and uniformly sized hepatocytes. Aggregation of inflammatory cells could not be seen. In the model group, the hepatic cells were disordered, with irregular cellular morphology. The cellular boundaries in this group were unclear. Cells appeared swollen and several cells exhibited incomplete nuclei, while a large number of cells presented inflammatory infiltration. AVP treatment appeared to promote order of hepatocytes and neatly arranged hepatic cords, protected the hepatocytes from damage and allowed the cell structure to remain clear in mice subjected to oxidative stress. The hepatic morphology of oxidative stress-treated mice became close to that of the normal group after AVP-H treatment.

As shown in Fig. 4, the spleen tissues of normal mice were complete, the corticomedullary junction was clear and the cells were neatly arranged. In the model group, the spleen structure was unclear as the shape had become irregular. The red medullary sinus had expanded and was filled with a large number of red cells. The white medullary lymphocytes were reduced in number when compared with the control group, with narrowed red medullary cords and sparsely arranged cells. AVP effectively alleviated the changes in spleen tissue

Table VI. Levels of NO, SOD, GSH-Px, GSH and MDA in the spleens of mice (n=10).

Group	NO (μmol/l)	SOD (U/ml)	GSH-Px (U/ml)	GS (mg/l)	MDA (nmol/ml)
Normal	1.56±0.06[b]	81.32±2.18[b]	117.59±8.06[b]	6.68±0.20[a]	0.55±0.07[b]
Model	8.71±0.23	18.24±0.89	38.93±1.48	2.00±0.15	4.70±0.15
Vc	5.52±0.12[a]	48.38±2.12[a]	69.69±3.27[a]	4.23±0.15[a]	2.13±0.07[a]
AVP-L	6.91±0.09[a]	28.87±1.18[a]	55.87±2.59[a]	3.21±0.15[a]	3.43±0.22[a]
AVP-H	4.20±0.16[a]	70.69±2.22[b]	92.62±2.67[b]	5.37±0.20[a]	1.12±0.05[a]

Values are presented as the mean ± standard deviation (N=10/group). [a]P<0.05 and [b]P<0.01 vs. the model group. Vc, mice treated with Vc (100 mg/kg); AVP-L, mice treated with low concentration of AVP (50 mg/kg); AVP-H, mice treated with a high concentration of AVP (100 mg/kg). AVP, *Apocynum venetum* polyphenol extract; GSH, glutathione; GSH-Px, glutathione peroxidase; MDA, malondialdehyde; NO, nitric oxide; SOD, superoxide dismutase; Vc, vitamin C.

Table VII. Levels of NO, SOD, GSH-Px, GSH and MDA in the brains of mice (n=10).

Group	NO (μmol/l)	SOD (U/ml)	GSH-Px (U/ml)	GS (mg/l)	MDA (nmol/ml)
Normal	4.62±0.21[b]	127.26±6.32[b]	166.39±7.52[b]	13.89±0.45[b]	0.42±0.11[b]
Model	12.50±0.61	35.10±1.25	41.10±2.49	2.17±0.18	6.32±0.43
Vc	7.15±0.19[a]	79.36±2.89[a]	115.25±5.88[a]	8.33±0.37[a]	1.57±0.10[a]
AVP-L	9.17±0.44[a]	61.25±3.05[a]	79.82±4.30[a]	4.29±0.31[a]	4.08±0.36[a]
AVP-H	6.03±0.32[a]	92.65±4.86[b]	137.86±5.38[b]	11.27±0.32[b]	0.79±0.12[b]

Values are presented as the mean ± standard deviation (N=10/group). [a]P<0.05 and [b]P<0.01 vs. the model group. Vc, mice treated with Vc (100 mg/kg); AVP-L, mice treated with low concentration of AVP (50 mg/kg); AVP-H, mice treated with a high concentration of AVP (100 mg/kg). AVP, *Apocynum venetum* polyphenol extract; GSH, glutathione; GSH-Px, glutathione peroxidase; MDA, malondialdehyde; NO, nitric oxide; SOD, superoxide dismutase; Vc, vitamin C.

morphology caused by D-galactose-induced oxidative stress and led to normal spleen morphology. The histomorphological observations of the skin, liver and spleen indicated that AVP could inhibit the histopathological changes caused by oxidation, and may serve a preventive and protective role. The effect of AVP exceeded that of the antioxidant Vc.

CAT, Cu/Zn-SOD and Mn-SOD expression in liver and spleen tissues of mice. As shown in Figs. 5 and 6, the expression levels of Cu/Zn-SOD, Mn-SOD and CAT were strongest in the liver and spleen tissues of mice in the control group compared with the other groups. Mice in the model group exhibited the opposite trend to the normal group; Cu/Zn-SOD, Mn-SOD and CAT expression was the lowest in the liver and spleen tissues of these mice compared with the other groups. After AVP and Vc administration, the expression levels of Cu/Zn-SOD, Mn-SOD and CAT were significantly increased in the liver and spleen tissues compared with the model group (P<0.05). Expression levels of these indicators in the liver and spleen tissues of oxidative stress-induced mice became close to those of normal mice after AVP-H treatment.

mRNA expression levels of neuronal nitric oxide synthase (nNOS), endothelial nitric oxide synthase (eNOS) and inducible nitric oxide synthase (iNOS) in the liver and spleen tissues of mice. As shown in Fig. 7, the mRNA expression levels of nNOS and eNOS in the liver and spleen tissues in the control group were significantly higher than those in the other groups (P<0.05), whereas iNOS expression was significantly lower compared with the other groups (P<0.05). D-galactose-induced oxidation significantly reduced nNOS and eNOS expression, and increased iNOS expression in the liver and spleen tissues of mice in the model group compared with the control group. AVP significantly inhibited the alterations in mRNA expression induced by D-galactose (P<0.05) and normalized mRNA expression in the liver and spleen tissues of oxidative stress-induced mice. The effect was better than that of Vc at the same concentration.

mRNA expression levels of heme oxygenase-1 (HO-1), nuclear factor-erythroid 2-related factor 2 (Nrf2), γ-glutamylcysteine synthetase (γ-GCS) and NAD(P)H quinone dehydrogenase 1 (NQO1) in the liver and spleen tissues of mice. As shown in Fig. 8, the mRNA expression levels of HO-1, Nrf2, γ-GCS and NQO1 in the liver and spleen tissues were significantly higher in the control group than those in the other groups (P<0.05), whereas mice in the model group exhibited the weakest mRNA expression levels in the liver and spleen tissues. The expression levels of HO-1, Nrf2, γ-GCS and NQO1 in the liver and spleen tissues of mice were significantly increased following treatment with AVP and Vc compared with the model group (P<0.05); the upregulating effect of AVP-H on these genes was stronger than that of AVP-L and Vc.

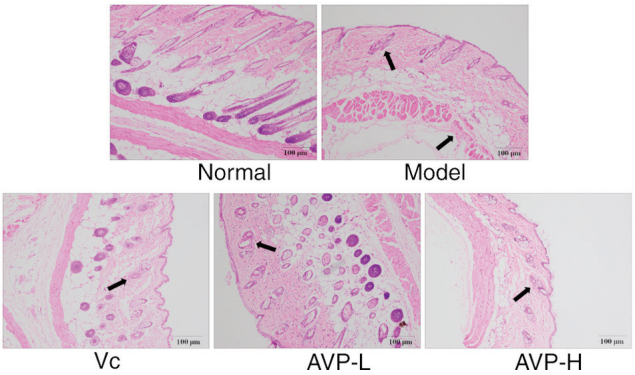

Figure 2. Hematoxylin and eosin staining of mouse skin. Magnification, x100. Vc, mice treated with 100 mg/kg Vc; AVP-L, mice treated with a low concentration (50 mg/kg) of AVP; AVP-H, mice treated with a high concentration (100 mg/kg) of AVP. AVP, *Apocynum venetum* polyphenol extract; Vc, vitamin C. Arrows indicate inflammed tissue.

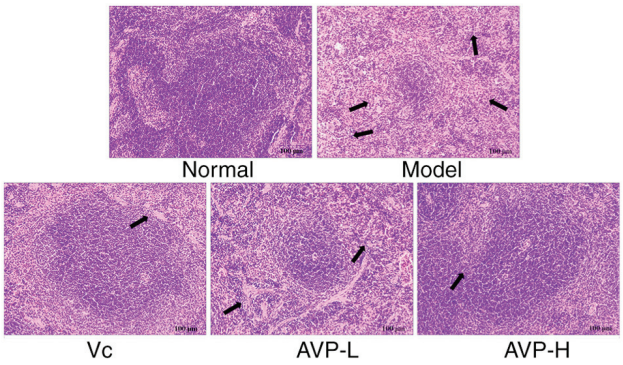

Figure 4. Hematoxylin and eosin staining of mouse spleen. Magnification, x100. Vc, mice treated with 100 mg/kg Vc; AVP-L, mice treated with a low concentration (50 mg/kg) of AVP; AVP-H, mice treated with a high concentration (100 mg/kg) of AVP. AVP, *Apocynum venetum* polyphenol extract; Vc, vitamin C. Arrow indicates inflammed tissue.

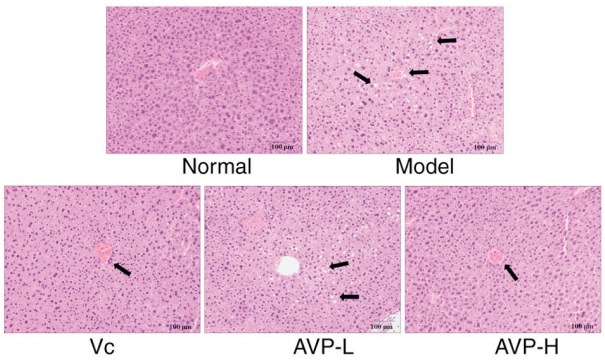

Figure 3. Hematoxylin and eosin staining of mouse liver. Magnification, x100. Vc, mice treated with 100 mg/kg Vc; AVP-L, mice treated with a low concentration (50 mg/kg) of AVP; AVP-H, mice treated with a high concentration (100 mg/kg) of AVP. AVP, *Apocynum venetum* polyphenol extract; Vc, vitamin C. Arrow indicates inflammed tissue.

Discussion

Organ weight and organ indices are indicators of the status of the animal body. Changes in organ weight and organ indices can reflect oxidative stress in the body; for example, when oxidative stress occurs, the thymus and brain will atrophy more obviously than other organs (20). The liver and kidneys are the main metabolic organs of mice. A decrease in organ weight and indices will directly affect the metabolic capacity of animals. Furthermore, the liver is also an important immune organ (17). A change in the hepatic index suggests that the immunity of the body has been affected (21). The spleen is related to the cellular immune system in the body and serves an important role in the immune mechanism. A decline in the quality of the spleen indicates atrophy of the organ, which can reduce its immune function (13). Therefore, determining the spleen index can directly reflect structural and functional changes in the organ, and therefore has importance for evaluating the successful establishment of a mouse model of oxidative stress (22). The results of this study indicated that D-galactose could reduce the organ indices of mice under oxidative stress and AVP could alleviate the decrease of organ indices caused by D-galactose, thus preventing oxidative stress in mice.

The increased release of excitatory amino acids, such as glutamic acid, activates NMDA receptors to induce Ca^{2+} influx. When intracellular Ca^{2+} concentration increases, activated NOS generates large amounts of NO, which accelerates Ca^{2+} influx and causes an overload of intracellular Ca^{2+}, directly inhibiting mitochondrial energy production. Furthermore, the generation of free radicals O_2^- and ·OH will be triggered, which aggravates the damage of brain cells (13). NO and O_2^- react with each other to form peroxynitrite anions that decompose into highly toxic OH^- and NO_2^-, which further accelerates cell death (23). Repeated infections in the body, even if not directly related to the central nervous system, can lead to synthesis of iNOS mRNA and can result in the production of a large amount of NO, which causes neuronal death in the hippocampus and memory damage, and accelerates the deterioration of aging neuronal lesions, such as those found in Alzheimer's disease (17). The synthesis of iNOS mRNA in the anterior pituitary and pineal glands produces NO, which can deteriorate the resistance to infections and reduce the production of melatonin, thus leading to brain aging (24). These studies support the hypothesis that the regulation of NO levels and the prevention of excessive NO serve a significant role in controlling aging. Studies have shown that eNOS in mouse aortic endothelial cells is significantly reduced under oxidative stress (17,19). eNOS can inhibit the aging of blood vessels caused by oxidative stress, as well as dilate and protect blood vessels (25). Under normal physiological conditions, the nervous system has mechanisms that precisely regulate NO production, release, diffusion and inactivation, mainly by regulating the activation and deactivation of nNOS. In addition to its important function in the nervous system, nNOS is also expressed in skeletal muscles, the myocardium and smooth muscle cells, where NO has an important role in regulating blood flow and muscle contraction (26). A decrease in the levels of nNOS leads to excessive NO production, which may lead to the occurrence of neurological diseases, such as cerebral ischemia injury, Alzheimer's disease and Parkinson's disease (27). The results of the present study suggested that AVP may possess the ability to influence the levels of NO, nNOS, eNOS and iNOS, helping to maintain these at normal

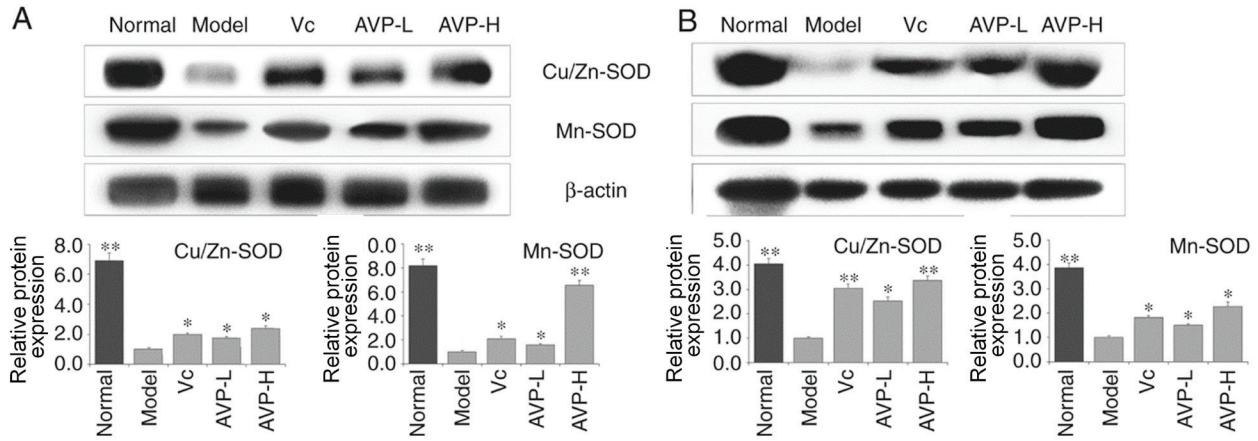

Figure 5. Cu/Zn-SOD and Mn-SOD protein expression in the (A) liver and (B) spleen of mice. *P<0.05 and **P<0.01 vs. the model group. Vc, mice treated with 100 mg/kg Vc; AVP-L, mice treated with a low concentration (50 mg/kg) of AVP; AVP-H, mice treated with a high concentration (100 mg/kg) of AVP. AVP, *Apocynum venetum* polyphenol extract; SOD, superoxide dismutase; Vc, vitamin C.

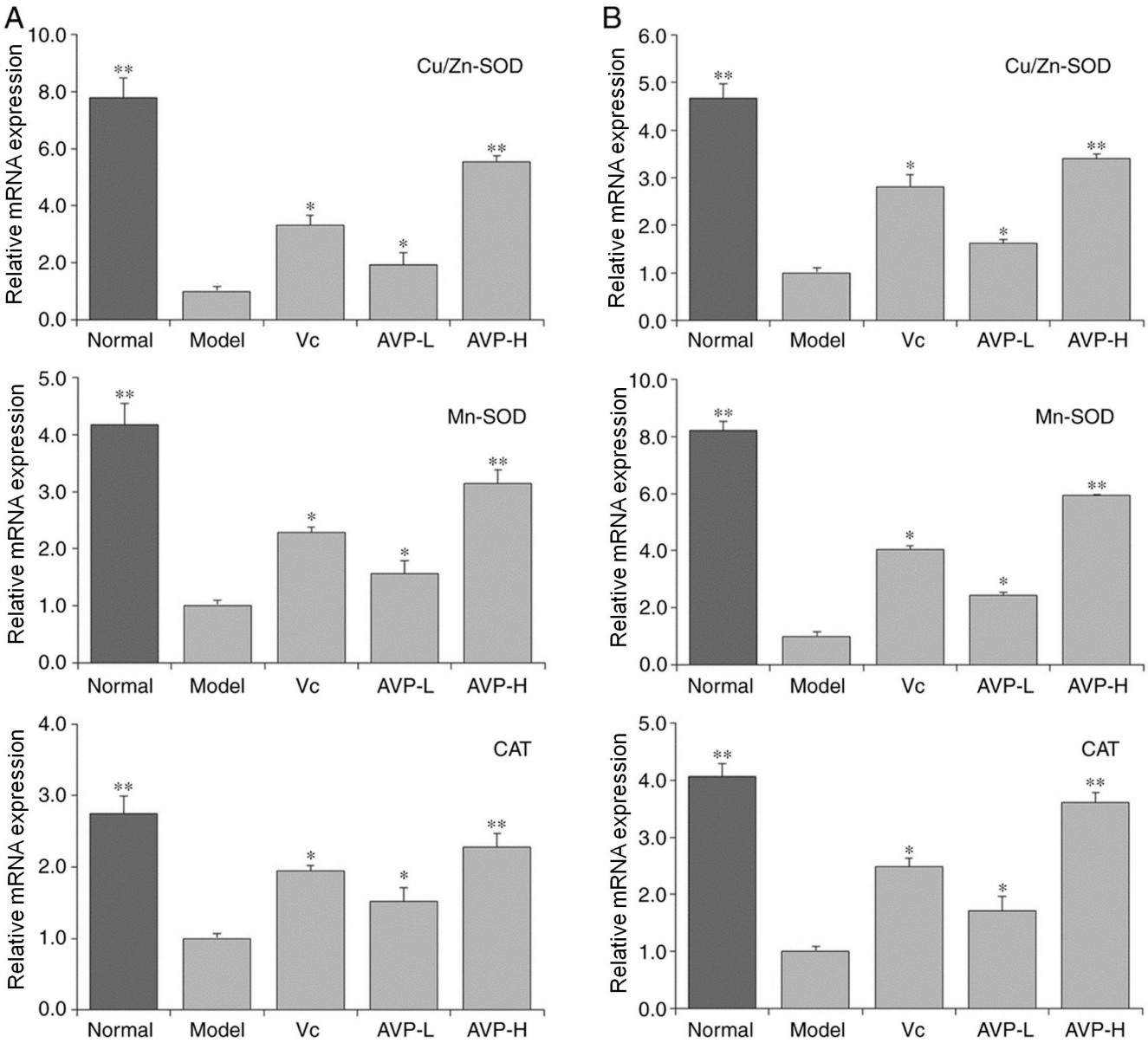

Figure 6. Cu/Zn-SOD, Mn-SOD and catalase mRNA expression in the (A) liver and (B) spleen of mice. *P<0.05 and **P<0.01 vs. the model group. Vc, mice treated with 100 mg/kg vitamin C; AVP-L, mice treated with a low concentration (50 mg/kg) of AVP; AVP-H, mice treated with a high concentration (100 mg/kg) of AVP. AVP, *Apocynum venetum* polyphenol extract; SOD, superoxide dismutase; Vc, vitamin C.

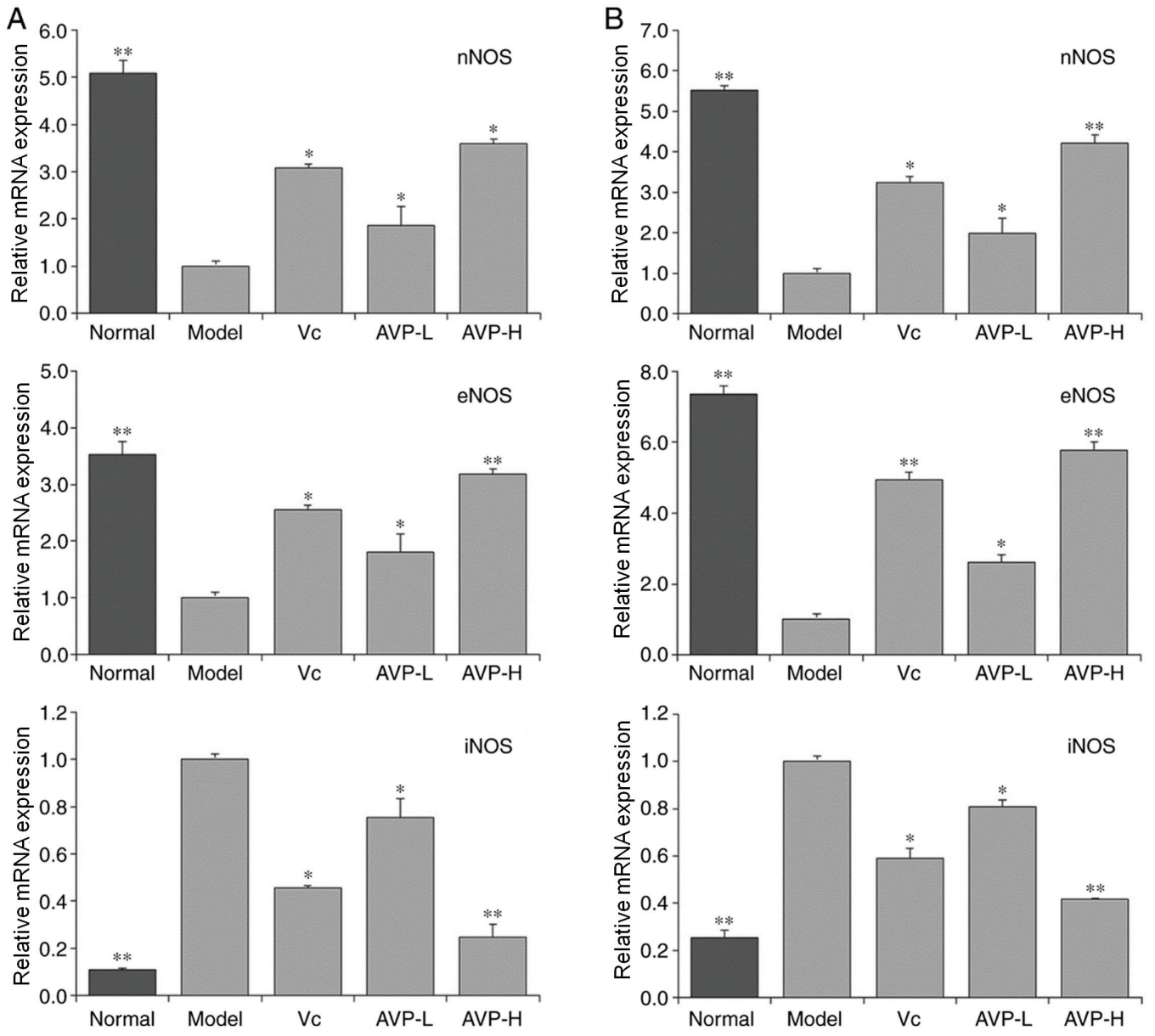

Figure 7. nNOS, eNOS and iNOS mRNA expression in the (A) liver and (B) spleen of mice. *P<0.05 and **P<0.01 vs. the model group. Vc, mice treated with 100 mg/kg Vc; AVP-L, mice treated with a low concentration (50 mg/kg) of AVP; AVP-H, mice treated with a high concentration (100 mg/kg) of AVP. AVP, *Apocynum venetum* polyphenol extract; eNOS, endothelial NOS; iNOS, inducible NOS; nNOS, neuronal NOS; NOS, nitric oxide synthase; Vc, vitamin C.

levels and to avoid an imbalance of NO, nNOS, eNOS and iNOS due to oxidative stress.

SOD is a type of metal enzyme widely distributed throughout the biological world. It is a key line of defense against reactive oxygen species. SOD can be generally divided into three types depending on the metal co-factors: Cu/Zn-SOD, Mn-SOD and Fe-SOD. Cu/Zn-SOD is an enzyme that can be predominantly found in the cytoplasm and chloroplast matrix of eukaryotic cells. In addition, Cu/Zn-SOD is present in the blood and viscera of animals (17). Mn-SOD predominantly exists in prokaryotic cells, eukaryotic cells and the mitochondrial matrix, whereas Fe-SOD mainly exists in prokaryotic cells and plants (26). SOD has an effective role in the prevention and treatment of diseases associated with superoxide free radicals. When in excess, superoxide anion radicals cause oxidative stress; in addition, when SOD concentration is low, oxidative stress may be induced (27). Levels of Cu/Zn-SOD and Mn-SOD decrease when the body is under oxidative stress (28). CAT is an antioxidant enzyme, which is abundant in erythrocytes, the cells of numerous tissue types, mitochondria and the cytoplasm (29). During normal oxidative respiration, organisms constantly produce reactive oxygen species, which contain unpaired electrons, and can be removed by CAT, SOD, GSH-Px and other enzymatic systems. As the first line of defense against reactive oxygen species, SOD converts O_2^- into H_2O_2, whereas CAT increases the cellular oxygen content by catalyzing the decomposition of H_2O_2 into H_2O (30). GSH is an important antioxidant in mammals that can scavenge free radicals produced in cells, thus alleviating cell membrane damage caused by the formation of reactive oxygen species during lipid peroxidation (31). GSH is either directly or indirectly involved in numerous microbial cell activities. Notably, GSH is able to build a strong defense against oxida-

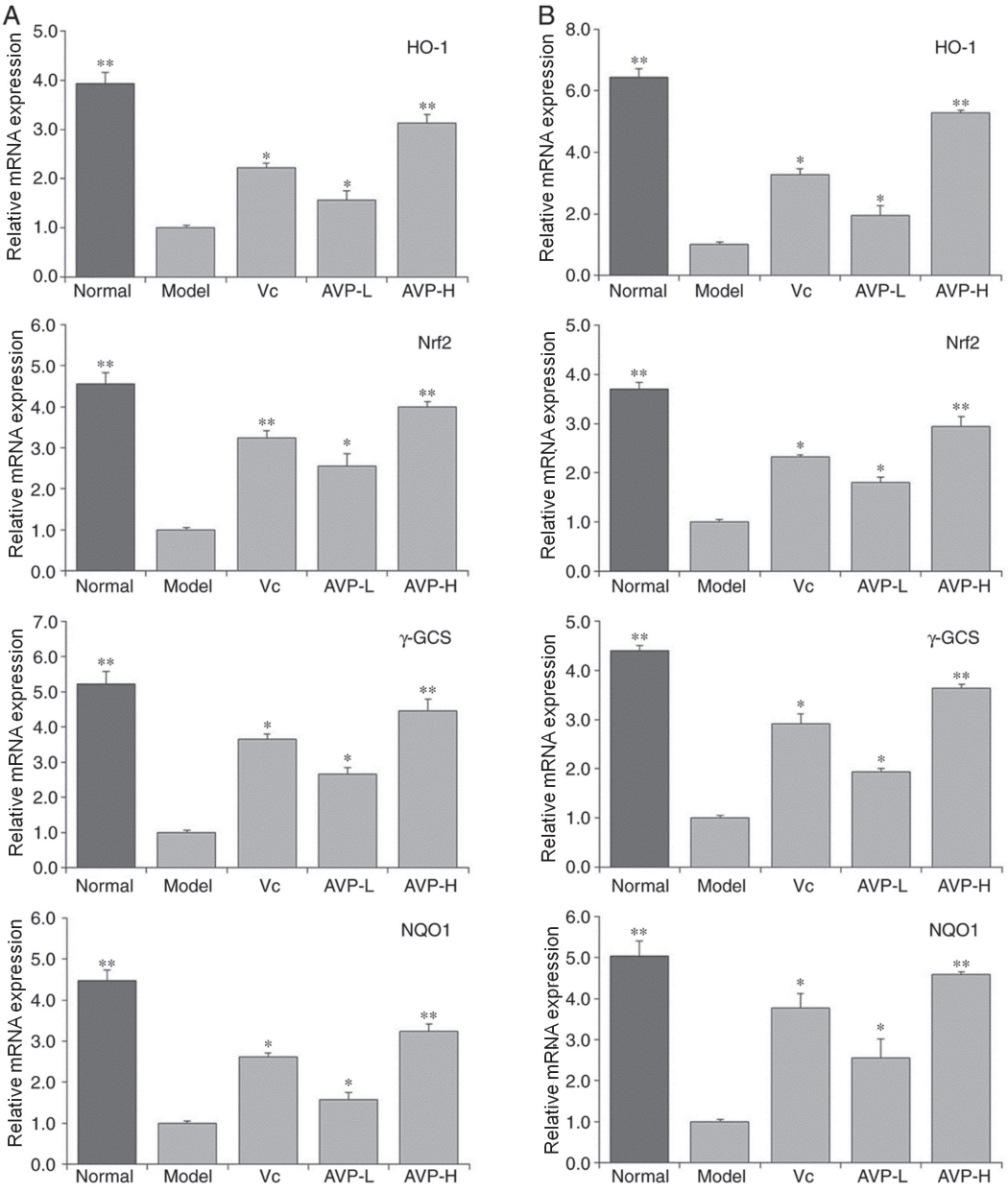

Figure 8. HO-1, Nrf2, γ-GCS and NQO1 mRNA expression in the (A) liver and (B) spleen of mice. *P<0.05 and **P<0.01 vs. the model group. Vc, mice treated with 100 mg/kg Vc; AVP-L, mice treated a low concentration (50 mg/kg) of AVP; AVP-H, mice treated with a high concentration (100 mg/kg) of AVP. γ-GCS, γ-glutamylcysteine synthetase; AVP, *Apocynum venetum* polyphenol extract; HO-1, heme oxygenase-1; Nrf2, nuclear factor-erythroid 2-related factor 2; NQO1, NAD(P)H quinone dehydrogenase 1; Vc, vitamin C.

tive stress together with related metabolic enzymes. One of the GSH reductions is composed of γ-glutamate-cysteine ligase (GSH1), GSH synthetase (GSH2), GSH reductase, GSH-Px and NADPH. The interaction of various factors in the system can inhibit oxidative stress and slow down oxidation (32) MDA is a lipid peroxide formed by oxidation; the levels of MDA *in vivo* directly reflect the degree of oxidation (33). In this study, AVP significantly regulated the oxidation, increased the levels of SOD, CAT, GSH (GSH1 and GSH2) and GSH-Px, and reduced the levels of MDA, thus effectively alleviating oxidative stress caused by D-galactose in mice.

As a stress protein, HO-1 is involved in anti-inflammatory and antioxidative processes, in addition to heme metabolism, and exerts strong protective effects on the cardiovascular and nervous systems. It has been reported that HO-1 has an antioxidant efficacy in vascular diseases, such as atherosclerosis, myocardial ischemic injury and hypertension, as well as neurological diseases, such as Alzheimer's disease, Parkinson's disease and cerebral ischemic injury (34). Nrf2 is important for the integrity of the vascular endothelium. A decline in Nrf2 function under oxidative stress is closely associated with the dysfunction of vascular endothelial cells. When the level of oxidative stress increases, Nrf2 is dissociated to promote the transcription and expression of HO-1, SOD and CAT, thus improving the ability to scavenge oxygen free radicals in the body (35). Nrf2 also has the function of regulating γ-GCS. Nrf2 is activated and promotes the expression of γ-GCS when a large quantity of reactive oxygen species is generated, and γ-GCS stimulates the synthesis and activation of GSH, which exerts an antioxidant role (36).

When cells are subjected to oxidative stress, Nrf2 can uncouple from Keapl, which can be activated and transferred into the nucleus, bind to antioxidant response elements, regulate the expression of the downstream antioxidant enzyme gene NQO1, and enhance the tolerance of cells to oxidative stress. The Nrf2/NQO1 signaling pathway is known to be associated with oxidative stress, and active substances can exert their antioxidative effects by regulating the Nrf2/NQO1 signaling pathway (37). In this study, AVP could upregulate the expression levels of oxidized Nrf2, and further enhance the expression of HO-1, γ-GCS and NQO1, thus protecting oxidized mice and preventing oxidative stress.

Phenolic compounds have phenolic hydroxyl groups, so they have a strong antioxidant effect, the phenolic hydroxyl group can provide hydrogen to react with free radicals to form inert products or more stable free radicals, thus interrupting or slowing down the chain reaction of free radicals (38). Studies have shown that the antioxidant activity of polyphenol is much better in a number of plants than that of Vc (39-41). The difference in the antioxidant activity of plant polyphenol is not only due to the molecular structure, but also due to the different three-dimensional conformation (42,43). *A. venetum* contains the active substance of AVP that has a strong antioxidant effect. This study also confirmed that the antioxidant effect of AVP was stronger than that of Vc at the same concentration; therefore, *A. venetum* could serve a preventive role against oxidative stress with its active ingredient AVP.

Neochlorogenic acid and chlorogenic acid are found in numerous types of TCM, and are reported to be beneficial in TCM treatment of inflammation and diabetes (44,45). Chlorogenic acid has also been suggested to have an inhibitory effect on lung cancer, gastric cancer and colon cancer (46,47). In addition to the suggestion that it has anticancer effects, rutin is believed to enhance the anticancer effect of other drugs and active substances (oxaliplatin, paeonol) used in TCM (48,49). *In vitro* studies have indicated that isoquercetin has inhibitory effect on gastric cancer cell proliferation (50,51). Astragalin and rosmarinic acid have been suggested to possess antioxidant activity and are bioactive substances (52,53). AVP contains neochlorogenic acid, chlorogenic acid, rutin, isoquercitrin, astragalin and rosmarinic acid. It is unclear whether the effect of the mixture of these six substances is due to their respective effective effects or combined effects, and further research is needed to clarify their underlying mechanism of action.

The results of the present study suggested that AVP may prevent D-galactose-induced oxidation in mice, and may return serum, skin, liver and spleen indices of mice under oxidative stress to close to their normal state. This effect was stronger than that of the well-known antioxidant Vc. *In vivo* experiments suggested that AVP is worthy of further study. The present preliminary study has begun to elucidate the mechanism of AVP activity; however, further human studies are required to verify its precise mechanism. In addition, the specific chemical composition of AVP needs to be further studied to clarify the direct relationship between the efficacy of AVP and its components.

Acknowledgements

Not applicable.

Funding

This research was funded by Chongqing scientific research institute performance incentive guidance project (cstc2018jxjlX0003), China.

Availability of data and materials

The datasets used and/or analyzed during the present study are available from the corresponding author on reasonable request.

Authors' contributions

JZ and XZ performed the experiments. PP and JY designed and directed the experiments. HG and ZK fed the animals, performed the experiments and wrote the manuscript. All authors approved the final manuscript for publication.

Ethics approval and consent to participate

This study followed a protocol approved by the Animal Ethics Committee of Chongqing Collaborative Innovation Center for Functional Food (approval no. 200802002B).

Patient consent for publication

Not applicable.

Competing interests

The authors declare that they have no competing interests.

References

1. Grundmann O, Nakajima J, Seo S and Butterweck V: Anti-anxiety effects of *Apocynum venetum* L. in the elevated plus maze test. J Ethnopharmacol 110: 406-411, 2007.
2. Tan X and Peng Y: Research progress of *Apocynum venetum* tea. Mod Chinese Med 16: 666-673, 2014.
3. Kim DW, Yokozawa T, Hattori M, Kadota S and Namba T: Inhibitory effects of an aqueous extract of *Apocynum venetum* leaves and its constituents on Cu(2+)-induced oxidative modification of low density lipoprotein. Phytother Res 14: 501-504, 2000.
4. Xiong Q, Fan W, Tezuka Y, Adnyana IK, Stampoulis P, Hattori M, Namba T and Kadota S: Hepatoprotective effect of *Apocynum venetum* and its active constituents. Planta Med 66: 127-133, 2000.
5. Xie W, Zhang X, Wang T and Hu J: Botany, traditional uses, phytochemistry and pharmacology of *Apocynum venetum* L. (Luobuma): A review. J Ethnopharmacol 141: 1-8, 2012.
6. Buford TW: Hypertension and aging. Ageing Res Rev 26: 96-111, 2016.
7. Chard S, Harris-Wallace B, Roth EG, Girling LM, Rubinstein R, Reese AM, Quinn CC and Eckert JK: Successful aging among african american older adults with type 2 diabetes. J Gerontol B Psychol Sci Soc Sci 72: 319-327, 2017.
8. Kitada M, Ogura Y and Koya D: The protective role of Sirt1 in vascular tissue: Its relationship to vascular aging and atherosclerosis. Aging (Albany NY) 8: 2290-2307, 2016.
9. Rao KS: Free radical induced oxidative damage to DNA: Relation to brain aging and neurological disorders. Indian J Biochem Biophys 46: 9-15, 2009.
10. Hohensinner PJ, Kaun C, Ebenbauer B, Hackl M, Demyanets S, Richter D, Prager M, Wojta J and Rega-Kaun G: Reduction of premature aging markers after gastric bypass surgery in morbidly obese patients. Obes Surg 28: 2804-2810, 2018.

11. Li L, Xu M, Shen B, Li M, Gao Q and Wei SG: Moderate exercise prevents neurodegeneration in D-galactose-induced aging mice. Neural Regen Res 11: 807-815, 2016.
12. Qian Y, Zhang J, Zhou X, Yi R, Mu J, Long X, Pan Y, Zhao X and Liu W: Lactobacillus plantarum CQPC11 isolated from Sichuan pickled cabbages antagonizes d-galactose-induced oxidation and aging in mice. Molecules 23: pii: E3026, 2018.
13. Li HY, Xia JQ, Yang LY and Zhong RZ: Plant polyphenols: Antioxidant capacity and application in animal production. China J Anim Nutr 25: 2529-2534, 2013.
14. Carluccio MA, Siculella L, Ancora MA, Massaro M, Scoditti E, Storelli C, Visioli F, Distante A and De Caterina R: Olive oil and red wine antioxidant polyphenols inhibit endothelial activation: Antiatherogenic properties of Mediterranean diet phytochemicals. Arterioscler Thromb Vasc Biol 23: 622-629, 2003.
15. Sharma S, Rana S, Patial V, Gupta M, Bhushan S and Padwad YS: Antioxidant and hepatoprotective effect of polyphenols from apple pomace extract via apoptosis inhibition and Nrf2 activation in mice. Hum Exp Toxicol 35: 1264-1275, 2016.
16. Delwing-Dal Magro D, Roecker R, Junges GM, Rodrigues AF, Delwing-de Lima D, da Cruz JGP, Wyse ATS, Pitz HS and Zeni ALB: Protective effect of green tea extract against proline-induced oxidative damage in the rat kidney. Biomed Pharmacother 83: 1422-1427, 2016.
17. Pan Y, Long X, Yi R and Zhao X: Polyphenols in Liubao tea can prevent CCl_4-induced hepatic damage in mice through its antioxidant capacities. Nutrients 10: 1280, 2018.
18. Livak KJ and Schmittgen TD: Analysis of relative gene expression data using real-time quantitative PCR and the 2(-Delta Delta C(T)) method. Methods 25: 402-408, 2001.
19. Li GJ, Wang J, Cheng YJ, Tan X, Zhai YL, Wang Q, Gao FJ, Liu GL, Zhao X and Wang H: Prophylactic effects of polymethoxyflavone-rich orange peel oil on N^{ω}-Nitro-L-arginine-induced hypertensive rats. Appl Sci 8: 752, 2018.
20. Tang T and He B: Treatment of D-galactose induced mouse aging with Lycium barbarum polysaccharides and its mechanism study. Afr J Tradit Complement Altern Med 10: 12-17, 2013.
21. Khan SS, Singer BD and Vaughan DE: Molecular and physiological manifestations and measurement of aging in humans. Aging Cell 16: 624-633, 2017.
22. Manini TM: Energy expenditure and aging. Ageing Res Rev 9: 1, 2010.
23. Tessari P: Nitric oxide in the normal kidney and in patients with diabetic nephropathy. J Nephrol 28: 257-268, 2015.
24. Wells SM and Holian A: Asymmetric dimethylarginine induces oxidative and nitrosative stress in murine lung epithelial cells. Am J Respir Cell Mol Biol 36: 520-528, 2007.
25. Fukai T, Siegfried MR, Ushio-Fukai M, Cheng Y, Kojda G and Harrison DG: Regulation of the vascular extracellular superoxide dismutase by nitric oxide and exercise training. J Clin Invest 105: 1631-1639, 2000.
26. Bonthius DJ Jr, Winters Z, Karacay B, Bousquet SL and Bonthius DJ: Importance of genetics in fetal alcohol effects: Null mutation of the nNOS gene worsens alcohol-induced cerebellar neuronal losses and behavioral deficits. Neurotoxicology 46: 60-72, 2015.
27. Lee MH, Hyun DH, Jenner P and Halliwell B: Effect of proteasome inhibition on cellular oxidative damage, antioxidant defences and nitric oxide production. J Neurochem 78: 32-41, 2001.
28. Kosenko EA, Tikhonova LA, Alilova GA, Montoliu C, Barreto GE, Aliev G and Kaminsky YG: Portacaval shunting causes differential mitochondrial superoxide production in brain regions. Free Radic Biol Med 113: 109-118, 2017.
29. Selvaratnam JS and Robaire B: Effects of aging and oxidative stress on spermatozoa of superoxide-dismutase 1- and catalase-null mice. Biol Reprod 95: 60, 2016.
30. Pawlak W, Kedziora J, Zolynski K, Kedziora-Kornatowska K, Blaszczyk J, Witkowski P and Zieleniewski J: Effect of long term bed rest in men on enzymatic antioxidative defence and lipid peroxidation in erythrocytes. J Gravit Physiol 5: P163-P164, 1998.
31. Berndt C and Lillig CH: Glutathione, glutaredoxins, and iron. Antioxid Redox Signal 27: 1235-1251, 2017.
32. Vázquez-Medina JP, Zenteno-Savín T, Forman HJ, Crocker DE and Ortiz1 RM: Prolonged fasting increases glutathione biosynthesis in postweaned northern elephant seals. J Exp Biol 214: 1294-1299, 2011.
33. Hosen MB, Islam MR, Begum F, Kabir Y and Howlader MZ: Oxidative stress induced sperm DNA damage, a possible reason for male infertility. Iran J Reprod Med 13: 525-532, 2015.
34. Sue YM, Cheng CF, Chang CC, Chou Y, Chen CH and Juan SH: Antioxidation and anti-inflammation by haem oxygenase-1 contribute to protection by tetramethylpyrazine against gentamicin-induced apoptosis in murine renal tubular cells. Nephrol Dial Transplant 24: 769-777, 2009.
35. Hong C, Cao J, Wu CF, Kadioglu O, Schüffler A, Kauhl U, Klauck SM, Opatz T, Thines E, Paul NW and Efferth T: The Chinese herbal formula Free and Easy Wanderer ameliorates oxidative stress through KEAP1-NRF2/HO-1 pathway. Sci Rep 7: 11551, 2017.
36. Iwayama K, Kusakabe A, Ohtsu K, Nawano T, Tatsunami R, Ohtaki KI, Tampo Y and Hayase N: Long-term treatment of clarithromycin at a low concentration improves hydrogen peroxide-induced oxidant/antioxidant imbalance in human small airway epithelial cells by increasing Nrf2 mRNA expression. BMC Pharmacol Toxicol 18: 15, 2017.
37. Jiang XP, Tang JY, Xu Z, Han P, Qin ZQ, Yang CD, Wang SQ, Tang M, Wang W, Qin C, *et al*: Sulforaphane attenuates di-N-butylphthalate-induced reproductive damage in pubertal mice: Involvement of the Nrf2-antioxidant system. Environ Toxicol 32: 1908-1917, 2017.
38. Wang SX, Li AM, Zhang JJ, Ou SY, Huang XS and Zhang GW: HPLC-ESI-MS analysis of phenolic compounds in different solvent fractions of ethanol extract of longan seeds and their antioxidant activities. Food Sci 32: 196-203, 2011.
39. Ramful D, Tarnus E, Aruoma OI, Bourdon E and Bahorun T: Polyphenol composition, vitamin C content and antioxidant capacity of Mauritian citrus fruit pulps. Food Res Int 44: 2088-2099, 2011.
40. Wittayarat M, Kimura T, Kodama R, Namula Z, Chatdarong K, Techakumphu M, Sato Y, Taniguchi M and Otoi T: Long-term preservation of chilled canine semen using vitamin C in combination with green tea polyphenol. Cryo Lett 33: 318-326, 2012.
41. Bai JW, Gao ZJ, Xiao HW and Wang XT: Polyphenol oxidase inactivation and vitamin C degradation kinetics of Fuji apple quarters by high humidity air impingement blanching. Int J Food Sci Technol 48: 1135-1141, 2013.
42. Yilixiati XKY and Li XJ: Inhibitory effect of epigallocatechin gallate on the proliferation of lewis lung cancer mice and A549 and Calu-3 lung cancer cells. Chin Pharm J 47: 585-589, 2012.
43. Shen SR, Jin CF, Yang XQ and Zhao BL: Study on the scavenging effects of EGCG and GCG on singlet oxygen with ESR method. J Tea Sci 20: 19-21, 2000.
44. Zhang LW, Ji T, Su SL, Shang RX, Guo S, Guo JM, Qian DW and Duan JA: Pharmacokinetics of Mori Folium flavones and alkaloids in normal and diabetic rats. Zhongguo Zhong Yao Za Zhi 42: 4218-4225, 2017 (In Chinese).
45. Hou N, Liu N, Han J, Yan Y and Li J: Chlorogenic acid induces reactive oxygen species generation and inhibits the viability of human colon cancer cells. Anticancer Drugs 28: 59-65, 2017.
46. Yamagata K, Izawa Y, Onodera D and Tagami M: Chlorogenic acid regulates apoptosis and stem cell marker-related gene expression in A549 human lung cancer cells. Mol Cell Biochem 441: 9-19, 2018.
47. Lukitasari M, Nugroho DA and Widodo N: Chlorogenic acid: The conceivable chemosensitizer leading to cancer growth suppression. J Evid Based Integr Med 23: 2515690X18789628, 2018.
48. Li Q, Ren LQ, Wang YD and Chen XX: Effects of rutin combined with oxaliplatin on the proliferation and apoptosis of human gastric cancer SGC-7901 cells. Chin J Clin Pharm Ther 22: 1099-1105, 2017.
49. Zhan P, Peng XS, Xu XM, Zhou YF, Zhang XP, He R and Zhou G: The anti-cancer study on combinating paeonol and rutin. Chin Arch Tradit Chin Med 28: 1710-1712, 2010.
50. Liu KY, Liu HJ, Wu JZ and Zhang TJ: Studies on inhibitory effect of active constituents from Tussilago farfara L. on lung cancer cells LA795 proliferation. J Fudan Univ (Nat Sci) 48: 125-129, 2009.
51. Li YY, Zhao SJ, Bai CZ, Zhang LW and Wang ZH: Effect of isoquercetin from Fagopyrum tataricum on the proliferation and apoptosis of human gastric carcinoma cell line SGC-7901. Food Sci 35: 193-197, 2014.
52. Kim MS and Kim SH: Inhibitory effect of astragalin on expression of lipopolysaccharide-induced inflammatory mediators through NF-κB in macrophages. Arch Pharm Res 34: 2101-2107, 2011.
53. Tepe B, Eminagaoglu O, Akpulat HA and Aydin E: Antioxidant potentials and rosmarinic acid levels of the methanolic extracts of Salvia verticillata (L.) subsp. Verticillataand S. verticillata (L.) subsp. Amasiaca (Freyn & Bornm.) Bornm. Food Chem 100: 985-989, 2007.